Review

Artificial Neural Networks and Gradient Boosted Machines Used for Regression to Evaluate Gasification Processes: A Review

Owen Sedej [†, ‡], Eric Mbonimpa[†, *, ‡], Trevor Sleight [‡], Jeremy Slagley [‡]

Department of Systems Engineering and Management, Air Force Institute of Technology, 2950 Hobson Way, WPAFB, USA; E-Mails: Owen.Sedej@afit.edu; Eric.Mbonimpa@afit.edu; trevor.sleight@afit.edu; jeremy.slagley@afit.edu

‡ Current Affiliation: Air Force Institute of Technology (AFIT)

† These authors contributed equally to this work.

* **Correspondence:** Eric Mbonimpa; E-Mail: Eric.Mbonimpa@afit.edu

Academic Editor: Islam Md Rizwanul Fattah

Special Issue: Control and Optimisation of Waste- to- Energy Systems

Abstract

Waste-to-Energy technologies have the potential to dramatically improve both the natural and human environment. One type of waste-to-energy technology that has been successful is gasification. There are numerous types of gasification processes and in order to drive understanding and the optimization of these systems, traditional approaches like computational fluid dynamics software have been utilized to model these systems. The modern advent of machine learning models has allowed for accurate and computationally efficient predictions for gasification systems that are informed by numerous experimental and numerical solutions. Two types of machine learning models that have been widely used to solve for quantitative variables that are of predictive interest in gasification systems are gradient boosted machines and artificial neural networks. In this article, the reviewed literature used either gradient boosted machines or artificial neural networks to successfully model gasification systems. The review of such literature allows for a comparison in machine

learning model architecture and resultant accuracy as well as an insight into what parameters are being used to inform the models and to make predictions.

Keywords

Machine learning models; gasification; artificial neural networks; gradient boosted machines

1. Introduction

Waste-to-Energy (WtE) technologies are of growing interest since they offer a multivariate solution to the sustainability dilemma: minimizing waste streams and returning both energy and materials. WtE technologies are typically categorized into thermal, biochemical, or mechanical processes. Previously, thermal technologies posed a number of adverse effects to the environment and human health, as poor-quality combustion can lead to the emission of undesirable pollutants such as NO_x, SO_x, dioxins, and furans. Fortunately, current advancements in combustion and air pollution control technologies have allowed thermal WtE technologies to achieve efficient energy and material recovery while minimizing adverse effects on the environment and human health [1].

Gasification is one of the most common alternatives to combustion as a means of proper thermal treatment of municipal solid waste (MSW) [2-5]. Gasification uses a thermal process coupled with a reduced oxygen environment of a reactor to convert the large molecules within MSW into small molecules [6-8]. Gasification is typically aided by the initial treatment of a high temperature combustion process of the MSW called pyrolysis. Through pyrolysis, a combustible gas known as a syngas is partially formed and primarily consists of H_2, CH_4, CO_2, and CO. Once finally treated in the gasification stage, the syngas can be used to generate energy. The different types of pyrolysis used with gasification are flash, fast, and slow [9]. Additionally, the reactors themselves have different configurations: fixed-bed, fluidized-bed, rotary kiln, ablative, and screw. Modern gasification systems have the ability to reduce the original MSW stream volume by 80-95% and achieve an exergy efficiency of up to 46.7% [10, 11].

Due to the complex nature of gasification systems, many different approaches have been taken to model these systems. Recently, traditional approaches like computational fluid dynamics (CFD) modeling and small-scale experiments have allowed for machine learning (ML) models to utilize data obtained by the previous research methods. This data then can build an accurate and easy-to-use model of gasification systems. ML models can make sense of the non-linear data attributed to the gasification process due to the wide range of varying system parameters such as temperature, MSW stream, pressure, heating rates, and reactor residence. By combining the available datasets of the parameters surrounding different gasification systems, ML models allow researchers to gain an accurate understanding of the nuanced system. ML models are becoming more popular within research surrounding gasification and WtE technologies, as they are much more cost-effective than experimental iterations. They also can achieve a higher accuracy than traditional CFD models.

ML models are used to solve for classification or regression prediction problems. Classification ML models create a mapping function by using input variables and discrete output variables. The output variables of classification ML models belong to a label or category, and thus, the mapping function is used to predict whether the outcome will be a label or category. Regression ML models

create a mapping function by using input variables and continuous output variables. The output variables of regression ML models are normally a real-value quantity; therefore, the mapping function is used to predict what the real-value quantity of the outcome is. ML regression models are useful for application with gasification systems because they are able to predict real-value system performance quantities such as syngas composition, remaining mass, lower heating value (LHV), and total syngas yield [11-15]. Two ML regression models that are commonly used with gasification systems are artificial neural networks (ANNs) and gradient boosted machines (GBMs). These machine learning methods were selected as they adapt well to complicated inputs/outputs as are commonly found with gasification technology and there was substantial literature available for consideration.

The purpose of this paper is to conduct a discussion of ANN and GBM ML models that are used with gasification systems. This discussion will first provide insight as to what gasification is and the key parameters that are used to describe the system, the literature that links ML models to gasification, and how the ANN and GBM models work. It will then analyze what statistical methods are used to evaluate the models and successful synthesis of gasification with ANN and GBM models that have been found in the literature.

2. Materials and Methods

This discussion focuses on gasification systems that are used for WtE processes and ML models, specifically ANNs and GBMs for regression, that are applied to these systems. This review contains 87 peer-reviewed journal articles. Searches for reviewed journal articles were conducted on databases such as ScienceDirect, IEEE Explore, Google Scholar, and SCOPUS. Search terms that were used to find reviewed journal articles consisted of the following key words: "Machine Learning", "Gasification", "Regression Analysis", "Neural Networks", "Gradient Boosted Machines".

3. Results and Discussion

3.1 The Gasification Process

Gasification is a thermal process in which a waste feedstock is decomposed into a syngas that can be used as a source of energy. The reaction that describes the conversion process of waste feedstock into the valuable syngas and other constituents is shown in Equation 1. The product syngas contains non-condensable gases such as H_2, CO, CO_2, H_2O, N_2, and some lighter hydrocarbons [16].

$$waste\ feedstock + heat \rightarrow syngas + tar + char + soot \qquad (1)$$
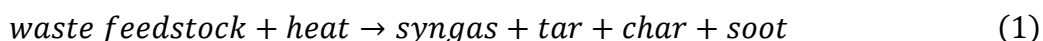
An elevated temperature must be applied in order to assist in the conversion from the input waste feedstock to a syngas. The typical temperature range in which gasification takes place is between 900-1500°C [17]. Some of the notable byproducts from the gasification process found in Equation 1 are tar and char. Tar consists of larger hydrocarbons that are a product of the gasification process and develop into a viscous substance [18]. Char consists of solids that are entrained within the product syngas and are composed of solid carbon and inorganic ash [19]. Char and tar byproducts should be minimized as they can lead to erosion, corrosion, and plugging of the gasification systems that can necessitate maintenance and decrease process efficiency [20].

Multiple process stages are employed to the gasification process in order to minimize the overall impact that char and tar have on the operational condition of the system. By using multiple stages, the waste feedstock can first be treated at a lower temperature (pyrolysis) allowing for initial char removal by the first reactor and cyclone before it enters the gasification reactor [21]. An example of a multi-stage gasification process and the separation of pyrolysis from gasification is illustrated in Figure 1. It is important to note that the tar is broken down to non-condensable gases in the final gasification step with the aid of oxygen [16]. Tar will be reduced to lighter hydrocarbons, hydrogen, and carbon monoxide in the final step process so that the heating value of tar will be retained within the product syngas [16].
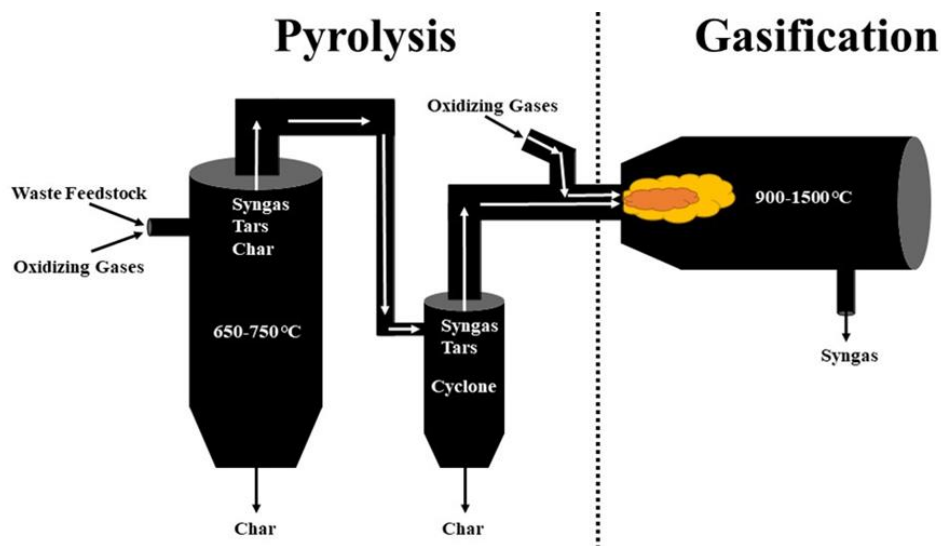

Figure 1 Schematic representation of a multi-stage gasification process.

The gasifier component of the multi-stage system can be classified by the parameters that describe the reactor. Fixed bed and fluidized bed reactors are two types of classifications based on the hydrodynamics of the gasification reactors. A fixed bed reactor holds the waste feedstock in relative place during the combustion process within the surrounding walls of the reactor [22]. A fluidized bed reactor allows the waste feedstock to move freely during the combustion process within the surrounding walls of the reactor [22]. Gasification reactors can be classified further based on the direction of flow within the reactor. In downdraft gasifiers, both the waste feedstock and any oxidating agent moves downward. However, in updraft gasifiers, the waste feedstock moves downward while the oxidating agents move upward [23]. Various types of commercial gasification reactors, their histories and classification based on chemical kinetics and hydrodynamics are found in the literature [24]. They have been used in diverse industries, such as fertilizer production, refineries, coal gasification, WTE, power generation, etc.

3.2 Important Gasification Process Terminology

It is important to know the terminology used to describe different parameters within the gasification process in order to understand how ML predictive models can be applied to these processes. This important terminology describes the inputs and outputs of the gasification system. Predicting the outputs of a gasification system from the inputs allows for the development of better

and more efficient systems. Table 1 defines the important terminology relevant to gasification systems.

Table 1 Important terminology describing the gasification process.

Term	Abbreviation	Description
Moisture Content	MC	The moisture content of the input waste feedstock (fuel) [25].
Lower Heating Value	LHV	The net heat of combustion [26]. Specifically relating to the created syngas.
Lower Heating Value of Products	LHV_p	The sum of the LHV of the syngas and the calorific value of entrained char and tar [11].
Reduction Zone Temperature	RZT	Portion of the gasifier directly above the combustion zone. This zone occurs once all the oxygen and gasifying media from the reaction is gone [27, 28]. In this zone the CO_2 and water vapor entrained by the gas flow have been reduced to CO and H_2 [27-29].
Equivalence Ratio	ER	The ratio of actual air fuel to the stoichiometric air fuel [30].
Injected Steam Ratio	ISR	The ratio of steam to dry feedstock [13].
Steam Flow Rate	SFR	Rate of steam flow input in (kg/h) [14].
Space Velocity	SV	The ratio of entering volumetric flow rate and the reactor volume [15].
Particle Size	None	Size of the entering waste feedstock [15].
Syngas Yield	GY	Yield of the syngas output [11].
Atmosphere Type	ATM	Level of CO_2 and N_2 within the reactor adjusted by experimental control [31].
Heating Rate	HR	The heating conditions within the reactor adjusted by experimental control [32].
Ash Content	A	Proximate analysis and resultant ash content of waste feedstock [33].
Gasifier Bottom Temperature	GBT	Temperature at the bottom of the gasification reactor [14].
Volatile Compounds	VC	Proximate analysis and resultant volatile compound content of waste feedstock [33].
Fixed Carbon	FC	Proximate analysis and resultant fixed carbon content of waste feedstock [33].

3.3 Machine Learning and Gasification Literature

Elsevier's abstract and citation database, Scopus, was used to scrub for articles using the Boolean search phrase: "Machine Learning" AND "Gasification". This Boolean search phrase returned 39 documents that contained both of the search terms within either their title, abstract, and keywords [34-72]. CitespaceV software used the data collected from the title, abstract, keywords, and references for each document. The software was able to visually model the interconnectedness of

matching key terms between the documents from the Scopus research database that used the Boolean search phrase. This visualization is shown in Figure 2. The visualization in Figure 2 utilized six different clusters to connect key terms that matched from the title, abstract, and keywords between the documents. The strength between the matching key terms is visualized by the thickness of each line that connects the individual document nodes. Matching key terms that appeared more frequently are visualized by a larger text font. Figure 2 exhibits that some of the stronger key terms were: "machine learning", "underground coal gasification", "artificial intelligence", "neural network", "regression analysis", and "artificial neural network". Furthermore, the color of the line between each node document indicates the year in which the document was published. The recency of the connection between ML models and gasification is demonstrated by the oldest document connecting these search terms being published in 2013. In fact, all the documents found in Scopus only have a nine-year timespan between the document with the earliest publication date and the latest.
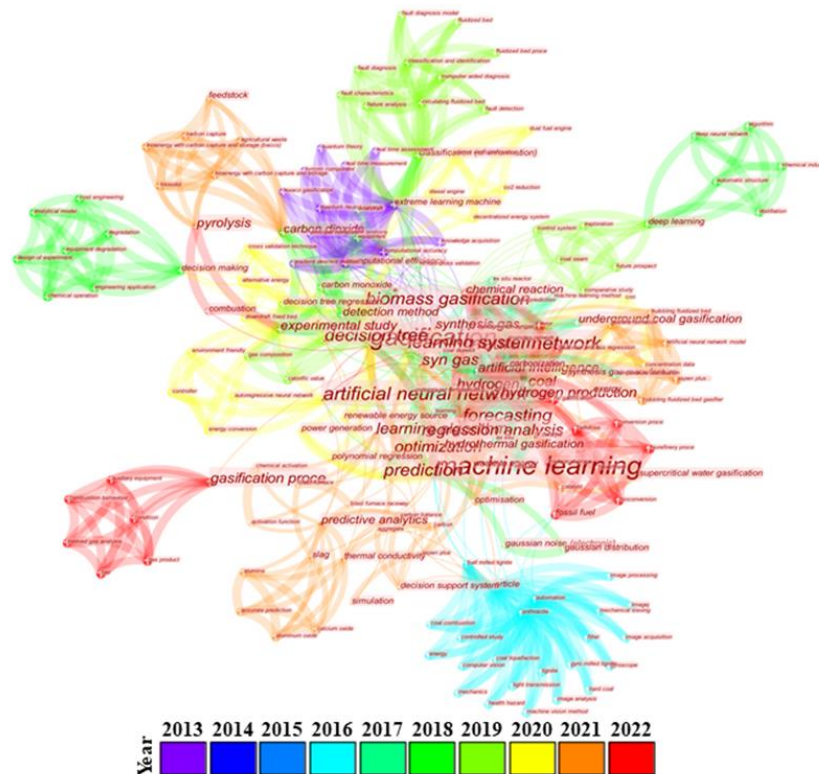

Figure 2 CitespaceV visualization network of matching key terms between Scopus documents.

3.4 ANN Models with Gasification

ANN models utilize available data in order to learn a process similar to the human brain. The advantage of ANN models over other types of theoretical and empirical models is that ANN models are universal approximators and therefore allow for close prediction accuracy in a variety of situations [11]. ANN models have been applied across a wide variety of fields including: weather prediction, signal processing, pattern recognition, function approximation, and process simulation [11]. Like many predictive models, the dataset that an ANN model utilizes to create its prediction is

typically a limiting factor of how accurate the ANN model predictions can get. Since the ANN model creates a unique predictive model based off the dataset it is fed, the more data that an ANN model can receive on the situation, then the more likely it will be representative of the non-linearities and "randomness" that exist within the dataset.

Two types of ANN architectures used for gasification modeling are a multilayer feed-forward neural network with multiple input and multiple output (MIMO) variables and multiple input and single output (MISO) model. Figure 3 shows a MIMO model with both dual and single layers. Both models shown in Figure 3 contain an input layer, a hidden layer or layers, and an output layer. When ANNs contain more than one hidden layer they are referred to as deep neural networks (DNNs) [73]. Beyond this basic description of neural networks in Figure 3, details about various neural network architectures can be found in previous studies [74]. Optimization of neural networks using genetic algorithms and particle swarm techniques were also presented [41, 75].
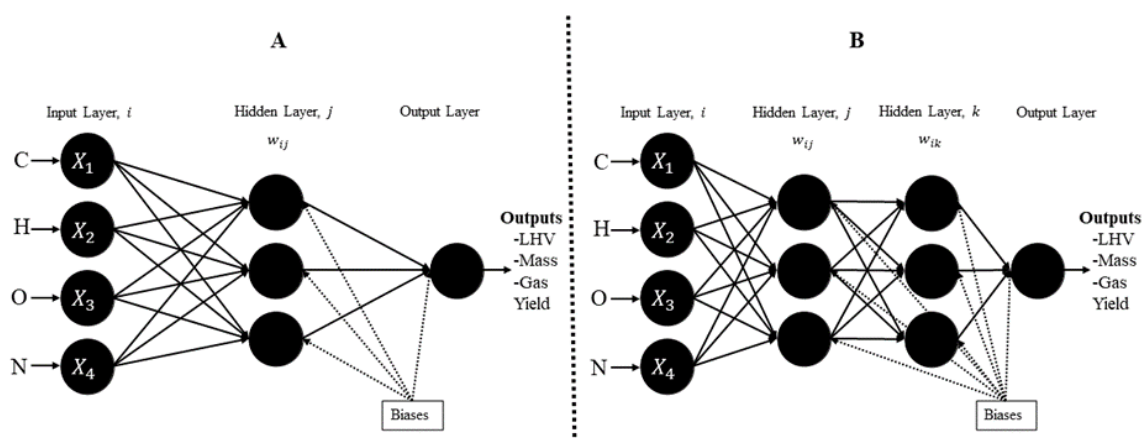

Figure 3 Schematic diagram of a MIMO ANN model (A) one hidden layer (B) two hidden layers.

The inputs and outputs of each layer are shown using typical parameters found in the literature used when modeling gasification. A range of all inputs used with gasification ANN models are shown in the "Input Parameters" column of Table 2 along with a range of all output parameters shown by the "Predictive Parameters" column. Table 2 also indicates the type of ANN model used in the "ANN model" column, the type of gasification process being modeled in the "System Description" column, and the number of layers in the ANN model in the "Number of Layers" column [41, 75].

Table 2 ANN models used with gasification.

Reactor Design	Model Details	Test Accuracy	Source
Plastic and rubber wastes	Multi-Layer Perceptron, 1-2 layers, 1 to 20 neurons	R^2 = 0.437 to 0.988	Ayodele et al, 2021 [38]
	Hidden Layer Function: standard and ordinary activation functions	Test/Val/Train%: 15/15/70 w/cross validation	
		Dataset Size: 30	

	Inputs: Temperature, Rubber seed shell particle size, HDPE particle size, Plastic % Outputs: Hydrogen Production (vol. %)	Epochs: 12	
Plastic and rubber wastes	Radial Basic Function, 1-2 layers, 1 to 20 neurons Hidden Layer Function: standard and ordinary activation functions	R^2 = 0.001 to 0.987 Test/Val/Train%: 15/15/70 w/cross validation	Ayodele et al, 2021 [38]
	Inputs: Temperature, Rubber seed shell particle size, HDPE particle size, Plastic % Outputs: Hydrogen Production (vol. %)	Dataset Size: 30 Epochs: 12	
Biomass in fixed bed downdraft gasifiers	MISO, 1 layer, 3-5 neurons Hidden Layer Function: tansig	R^2 = 0.9855 to 0.9928 RMSE = 0.0523 to 0.0915	Baruah et al, 2017 [12]
	Inputs: Carbon, Hydrogen, Oxygen, Ash Content, Moisture Content, and RZT Output: Producer Gas Composition (CO, CH_4, CO_2, and H_2)	Test/Train%: 30/70 w/cross validation Dataset Size: 63 Epochs: 1000	
Pyrolysis of cattle manure	MISO, 2 layers, 8/6 neurons Hidden Layer Function: Not reported	R^2 = 0.8040 (test set) RMSE = 0.8347 Test/Train%: 30/70 w/o cross validation	Cao et al, 2015 [76]
	Inputs: Heating Rate, Temperature, Holding Time, Moisture Content, Sample Mass Output: Biochar Mass	Dataset Size: 33 Epochs: not reported	
Biomass in fluidised bed gasifier, sawdust, coconut shell coffee husk, sugarcane	MISO, 1 layer, 15 neurons Hidden Layer Function: tansig Inputs: Equivalence ratio (air supplied to the stoichiometric air	R^2 = 0.987 MSE = 0.71 Test/Val/Train%: 15/15/70 w/o cross validation	George et al, 2018 [77]

bagasse, groundnut shell	requirement), Moisture Content, Ash Content, Temperature, Carbon, Hydrogen, Oxygen	Dataset Size: 70	
		Epochs: 40	
	Outputs: Producer Gas Yield, Producer Gas Composition (CO, CH_4, CO_2, and H_2)		
MSW in fluidized bed reactor	MISO, 1 layer, 8 neurons	R^2 = 0.8994 to 0.9925 MSE: 0.0077 to 0.0003	Pandey et al, 2016 [11]
	Hidden Layer Function: logsig		
		Test/Val/Train%: 15/15/70 w/cross validation	
	Inputs: Carbon, Hydrogen, Nitrogen, Sulfur, Oxygen, Moisture Content, Ash Content, Equivalence Ratio, Temperature		
		Dataset Size: 67	
	Output: LHV, LHVp (including tars and entrained char), Gas Yield	Epochs: 100	
MSW in fluidized bed reactor	MIMO, 1 layer, 28 neurons	R^2 = 0.9402 to 0.9905 MSE = 0.0031	Pandey et al, 2016 [11]
	Hidden Layer Function: logsig		
		Test/Val/Train%: 15/15/70 w/cross validation	
	Inputs: Carbon, Hydrogen, Nitrogen, Sulfur, Oxygen, Moisture Content, Ash Content, Equivalence Ratio, Temperature		
		Dataset Size: 67	
	Output: LHV, LHVp (including tars and entrained char), Gas Yield	Epochs: 100	
Biomass in circulating fluidized bed gasifiers	MISO, 1 layer, 2 neurons	R^2 < 0.98 RMSE = 0.093 to 0.332	Puig-Arnavat et al, 2013 [13]
	Hidden Layer Function: tansig		
		Test (also Val)/Train%: 20/80 w/o cross validation	
	Inputs: Ash Content, Moisture Content, Carbon, Hydrogen, Oxygen, Equivalence Ratio, Temperature		
		Dataset Size: 18	
	Output: Producer Gas Yield, Producer Gas Composition (CO, CH_4, CO_2, and H_2)	Epochs: not reported	
Biomass in bubbling fluidized bed gasifiers	MISO, 1 layer, 2 neurons	R^2 < 0.98 RMSE = 0.036 to 790	Puig-Arnavat et
	Hidden Layer Function: tansig		

		Test (also Val)/Train%: 20/80 w/o cross validation	al, 2013 [13]
	Inputs: Ash Content, Moisture Content, Carbon, Hydrogen, Oxygen, Equivalence Ratio, Temperature, Injected Steam Ratio	Dataset Size: 36	
	Output: Producer Gas Yield, Producer Gas Composition (CO, CH$_4$, CO$_2$, and H$_2$)	Epochs: not reported	
Downdraft biomass gasification integrated with power production unit	MISO, 1 layer, 40 neurons	R^2 = 0.999 RMSE = 0.46	Safarian et al, 2020 [78]
	Hidden Layer Function: tansig	Test/Train%: 30/70 w/o cross validation	
	Inputs: Moisture Content, Volatile Materials, Fixed Carbon, Ash Content, Carbon, Oxygen, Hydrogen, Nitrogen, Sulfur, Temperature. Air to Fuel Ratio	Dataset Size: 86 Epochs: not reported	
	Outputs: Power Output (Watts)		
Bubbling fluidized bed gasification	MISO: 2 layers, 1 to 30 neurons	R^2 = 0.89 to 0.97 MSE = 0.000444 to 0.00126	Serrano et al, 2020 [79]
	Hidden Layer Functions: tansig, logsig, purelin	Test/Train%: 20/80 w/o cross validation	
	Inputs: Carbon, Hydrogen, Oxygen, Moisture Content, Ash, Equivalence Ratio, Temperature, Bed Material, Steam/Biomass Mass Ratio	Dataset Size: 203 Epochs: 2000	
	Outputs: Producer Gas Composition (CO, CH$_4$, CO$_2$, and H$_2$), Gas Yield		
Supercritical water gasification, food waste	MISO, 1 layer, 3-7 neurons	R^2 = 0.98 to 0.99 MSE = 0.022 to 0.269	Shenbagaraj et al, 2021 [80]
	Hidden Layer Function: logsig	Test/Train%: 30/70	
	Inputs: Temperature, Residence Time, Feed Concentration	Dataset Size: 40	
	Outputs: Producer Gas Composition(CO, CH$_4$, CO$_2$, and H$_2$)	Epochs: 40	

Pyrolysis of pine sawdust	MIMO, 1 layer, 7 neurons Hidden Layer Function: Inputs: Space Velocity, Temperature, Particle Size Output: Producer Gas Yield, Producer Gas Composition (CO, CH_4, CO_2, and H_2)	R^2 = 0.999 MSE = 0.01 Test/Train%: 15/85 w/o cross validation Dataset size: not reported Epochs: not reported	Sun et al, 2016 [15]
Biomass	MISO, 1 layer, 20, 17 and 30 neurons (corresponding to the different outputs below) Hidden Layer Function: tansig Inputs: percent of cellulose, hemicellulose and lignin Outputs: kinetic parameters: activation energy, pre-exponential factor and reaction order	R^2 = 0.93 to 0.94 Test/Val/Train%: 15/15/70 w/o cross validation Dataset Size: 150 Epochs: not reported	Sunphorka et al, 2016 [81]
Downdraft fixed bed gasifier	Multiple Designs, 1 layer, 10 neurons Hidden Layer Function: tansig Inputs: Temperature Distribution, Air Flow Rate, Equivalence Ratio, Carbon, Hydrogen, Oxygen, Nitrogen, Moisture Content, Volatile matter, Fixed Carbon, Ash Content Outputs: Producer Gas Composition (CO, CH_4, CO_2, and H_2), LHV	R^2 = 0.95 to 0.99 RMSE = 0.1513 to 2.2985 Test/Val/Train%: 15/15/70 w/o cross validation Dataset Size: 10 case studies, (a total of 3831 individual data points) Epochs: 1000	Yucel et al, 2019 [82]
Pyrolysis of cattle manure	Multi-Layer Perceptron: 2 layers, 32 neurons per layer Hidden Layer Function: ReLU activation function Inputs: Heating Rate, Temperature	R^2 = 0.9995 RMSE = 0.602 Test/ Train%: 20/80 w/o cross validation	Zhang et al, 2019 [31]

	Outputs: Remaining Mass	Dataset Size: not reported
		Epochs: not reported

Where: MISO: Multiple Input Single Output, MIMO: Multiple Input Multiple Output, ReLu: Rectified Linear Unit, MSE: Mean Square Error, RSME: Root Mean Square Error.

In the ANN model, each neuron that is not in the input layer uses a non-linear transfer function when moving towards the output layer [11]. The transfer functions that have been utilized with gasification and ANN models found in the literature are shown in the "Transfer Function" column of Table 2. When the ANN models exceed a single hidden layer, they are able to utilize the same or different transfer function between each respective layer. Therefore, an ANN model that has two layers is able to use two of the same or different transfer functions. When the ANN model transitions from the final hidden layer to the output layer, all of the ANN models in the literature review used a pure linear transfer function. Table 2 shows that three different types of transfer functions have been used with ANN models predicting gasification. These three different types of transfer functions are a hyperbolic tangent sigmoid function (tansig), a logarithmic sigmoid function (logsig), and a rectified linear activation function (ReLU). The activation functions are shown in Equations 2, 3, and 4, respectively. Different transfer functions, and combinations thereof, can create different prediction accuracies for the same dataset. Therefore, it is important to iterate combinations of transfer functions when setting up an ANN model in order to find the best fit function for the gasification system.

$$\text{tansig: } f(x) = \frac{e^x - e^{-x}}{e^x + e^{-x}} \tag{2}$$

$$\text{logsig: } f(x) = \frac{1}{1 + e^{-x}} \tag{3}$$

$$\text{ReLU: } f(x) = \max(0, x) \tag{4}$$

The output of the MIMO ANN Model with a single hidden layer in Figure 3 is shown as y_j in Equation 5. In Equation 5, neurons, x_i, distribute the input signals to the hidden layer, j [11]. he neurons in hidden layers sum up the input signal x_i, after multiplying by the weight w_{ij}. f represents the activation function, d is the dimension of the network, l is the number of layers, and w_{ij}^l is the weight which belongs to the network with l layers and has i input and j hidden layers [11]. The MIMO ANN model with a single hidden layer in Figure 3 weights are described mathematically in Equation 6.

$$y_j = f\left(\sum_{i=0}^{d^{(l-1)}} \left(w_{ij}^l x_i^{l-1}\right)\right) \tag{5}$$

$$w_{ij}^l \in \begin{cases} 1 \le l \le L \; layers \\ 0 \le i \le d^{l-1} \; input \\ 1 \le j \le d^l \; output \end{cases} \tag{6}$$

Table 2 shows the number of neurons in the "Neurons" column and the different number of layers in the "Number of Layers" column for different ANN models. Once the ANN model has reached an output value y_{ij}, it then utilizes a training function to train the neural network to recognize an input and map to an output. All the research found in the literature review used the Levenberg-Marquardt back propagation algorithm (LMBPA) in order to train the neural network. This is shown in the "Training Function" column of Table 2. The LMBPA gives accurate results for moderate sized neural networks [11]. In tandem with a training function, the ANN model also uses a learning function in order to manipulate the individual weights and thresholds of the network. All the research found in the literature review showed that a gradient descent (GD) function was employed by the ANN model. This is shown in the "Learning Function" column in Table 2. Equation 7 shows the LMBPA where the Jacobian, J, is calculated using backpropagation, followed by the Hessian $H = J^T J$ and the gradient calculation ($g = J^t e$) where e is the network error [11]. In this function, μ is a scalar, and after each successful step, the value of μ is increased or decreased as determined by the cost function. The LMBPA minimizes the mean squared error (MSE) between the target output and the calculated output.

$$x_{k+1} = x_k - [J^T J + \mu I]^{-1} J^t e \tag{7}$$

In order to check the accuracy of the ANN model, the dataset is randomly divided into proportions for training, validation, and testing purposes. The proportions used for respective training, validation, and testing purposes by ANN models used to predict gasification systems are shown by the "Data Division" section in Table 2. Additionally, some ML models employed cross-validation within the network, allowing for the training, validation, and testing data to be re-split multiple times. This process finds the best representative model. Whether an ANN model that is predicting gasification systems used cross validation or not is shown in in Table 2. For consistency, only papers that used a form of waste as fuel (as opposed to a fossil fuel) were reviewed.

In papers where multiple models were considered, the parameters of the best performing model were included in Table 2. Interestingly, models with multiple hidden layers did not necessarily perform better than models with only one layer. Furthermore, in most cases good performance can be achieved with 10 or fewer neurons. Temperature, equivalence ratio and moisture content, were consistently important inputs [13, 76, 78], and in some models the carbon percentage was also important [78]. Temperature was particularly impactful for the hydrogen output [15, 80]. Gasifiers using a wide variety of different fuels including agricultural biomass, municipal solid waste, or industrial waste can be represented with these techniques. The most common output variables predicted were: Power Output (units varied) and Producer Gas Composition (typically: CO, CH_4, CO_2, and H_2).

3.5 GBM Models with Gasification

GBM ML models utilize available data as an efficient solving tool for regression problems that can make predictions for datasets with complex non-linearities [83]. The GBM ML model uses an ensemble of weak predictive learners, known as decision trees, to create an accurate predictive model. Each weak predictive learner corrects on the predecessor's error through a gradient descent function that is used to minimize the error and thus fit the model [84, 85]. An illustration of a gross

representation of the GBM process that shows how the model leverages an ensemble of weak predictive learners for a strong prediction tool is in Figure 4.
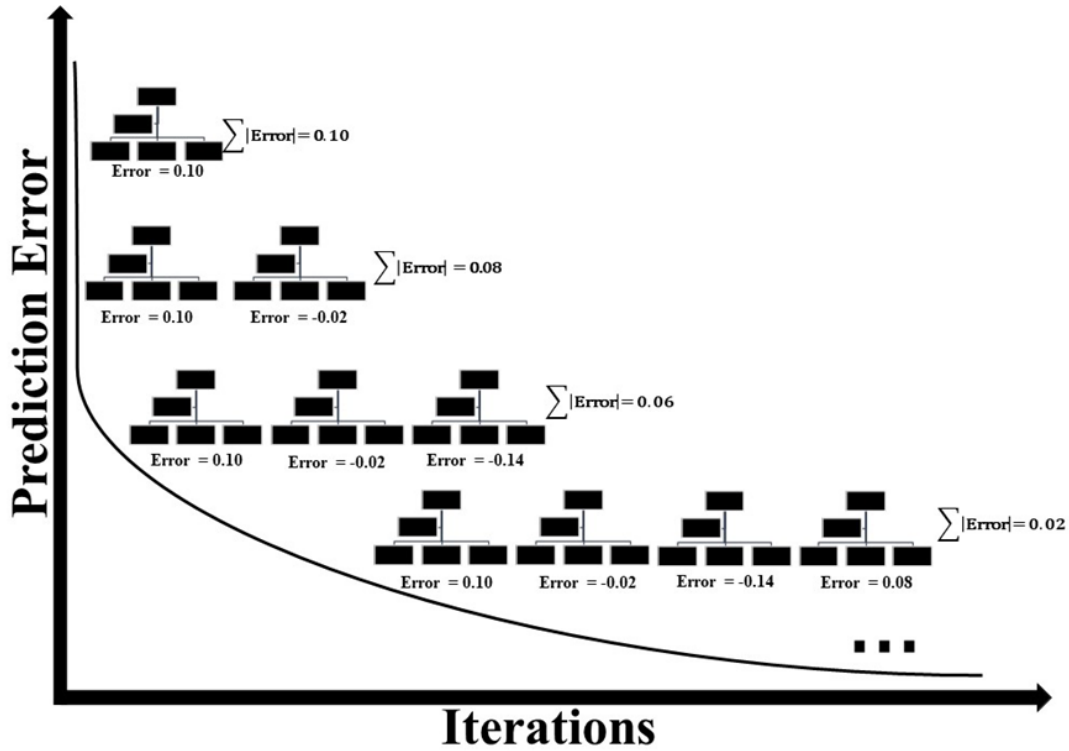

Figure 4 Gross representation of a GBM ML model method.

As shown in Figure 4, the GBM ML model minimizes the expected loss function through the use of decision trees [86]. The parameters of the GBM ML model include depth of trees, the learning rate, and the number of iterations [86]. The GBM algorithm is mathematically expressed as a summation of decision trees in Equation 8.

Generalized GBM model:

$$f_m(x) = \sum_{m=1}^{M} T(x, \theta_m), \qquad T(x, \theta_m) \tag{8}$$

θ_m is the parameter of the decision tree and M is the number of decision trees. A gradient descent loss function is then used by the GBM ML model in order to optimize the next parameter, shown in Equation 9 [84, 85].

GBM Loss Function:

$$\theta_{m+1} = \text{argmin} \sum_{t=1}^{N} L\big(y_t, F_m(x) + h(x, \theta_{m+1})\big) \tag{9}$$

Table 3 provides an overview of different GBM models for regression found in the literature that were used for prediction of gasification systems. Similar to ANN ML models, GBM models also split the dataset into proportions to be used for testing, training, and validation of the model.

Additionally, all GBM models used with gasification systems employed cross-validation within the algorithm in order to randomize the data multiple times and find the best-fit *m*.

Table 3 GBM ML models for regression used with gasification.

Reactor Design	Model Details	Test Accuracy	Source
Wet organic waste	GBR Inputs: Feedstock Composition, Operational Conditions, Outputs: Producer Gas Composition (CO, CH_4, CO_2, and H_2)	R^2 = 0.90 to 0.95, RMSE = 0.39 to 2.07	Li et al, 2020 [87]
Rice husks in fixed bed updraft gasifier	GBR Inputs: Equivalence Ratio, Bottom Temperature, Steam Flow rate Outputs: Producer Gas Composition (CO, CH_4, CO_2, H_2, and N_2)	R^2 = 0.59 to 0.78	Wen et al, 2021 [14]
Pyrolysis of algae	XGB Inputs: Elementary Feedstock Composition (Carbon, Hydrogen, Oxygen, and Nitrogen) Ratio of elementary composition (Hydrogen/Carbon, Oxygen/Carbon and Nitrogen/Carbon), Proximate Analysis; Ash content; Fixed carbon, Volatile Compound, Pyrolysis time, Heating rate, Temperature, Outputs: Biochar Yield	R^2 = 0.84	Pathy et al, 2020 [33]
Pyrolysis of cattle manure	GBR Inputs: Temperature, Heating Rate, Atmosphere Type Outputs: Remaining Mass	R^2 = 0.9989, RMSE = 0.820	Zhang et al, 2019 [31]
Pyrolysis of textile dyeing sludge and incense sticks	GBR Inputs: Blend Ratio, Heating Rate, Atmosphere Type, Temperature Outputs: Mean Remaining Mass Derivative Thermogravimetry and Differential Scanning Calorimetry	R^2 = 0.5978 to 0.9989 RMSE = 1.695 to 1.762	Wen et al, 2020 [32]

Where: GBR: Gradient Boosted Regression, XGB: eXtreme Gradient Boosted Regression.

The inputs to the GBR models were similar to the ANN models. A wider variety of different types of biowaste was use in the papers employing BGR modeling, which might account for some of the papers having lower metrics. However, good performance (R^2 and RSME) can also be achieved in most cases with GBR models. Of the models that included an analysis of the importance,

Temperature [14, 31-33] was consistently the most impactful predictor, with Heating Rate and Blend Ratio also having a significant contribution [31, 32].

3.6 Performance Evaluation of ANN and GBM ML Models

The error for the ANN and GBM ML models used for regression predictions of gasification systems can be found in the "Test Accuracy" columns in Table 2 and Table 3. The regression model accuracy for all the ML models in Table 2 and Table 3 utilize one or multiple of four evaluation metrics. These four types of evaluation metrics utilized by the ML models are the mean absolute error (MAE), the mean standard error (MSE), the root mean squared error (RMSE), and the coefficient of determination (R^2). They are described respectively by Equations 10, 11, 12, and 13. These evaluation metrics are calculated by comparing the output created by the ML model and comparing it to the expected real value output found in the dataset. In the following equations $Y_{predicted}$ is the value generated by the ML model, Y_{actual} is the expected value on the test dataset, and n is the number of iterations of the ML model.

$$MAE = \frac{1}{n}\sum_{i=1}^{n}|Y_{predicted} - Y_{actual}| \tag{10}$$

$$MSE = \frac{1}{n}\sum_{i=1}^{n}(Y_{predicted} - Y_{actual})^2 \tag{11}$$

$$RMSE = \sqrt{MSE} = \sqrt{\frac{1}{n}\sum_{i=1}^{n}(Y_{predicted} - Y_{actual})^2} \tag{12}$$

$$R^2 = 1 - \frac{\sum_{i=1}^{n}(Y_{actual} - Y_{predicted})^2}{\sum_{i=1}^{n}(Y_{actual} - Y_{mean\ value})^2} \tag{13}$$

Table 2 and Table 3 demonstrate how effective ML models can be to predict key performance parameters in gasification systems. These models achieved an R^2 value as high as 0.995, an RMSE value as low as 0.049, and an MSE as low as 0.0004.

4. Conclusions

ANN and GBM ML models for regression have been employed in numerous recent studies in order to make accurate predictions for gasification systems. The development of these ML models allows for better understanding and optimization of the gasification process. ML models allow for an alternative form of gasification system investigation than the traditional means of computational fluid dynamics modeling (CFD) or experimental iterations. There are many drawbacks to the traditional means of CFD modeling and experimental iterations to describe gasification systems. The former, CFD modeling, requires a high level of expertise, proper computing power, and can take a long time to create multiple modeling scenarios. The latter, experimental iterations, also requires a high level of expertise and can take a long time, but they additionally can have a high cost since

there must be a large investment into proper materials and data analysis equipment. ML models mitigate the issues surrounding CFD modeling and experimental iterations of gasification systems by combining existing iterations of these methods and synthesizing them into an accurate and specific algorithm. The advancement of integration of ML models into gasification and other WtE technologies will serve to speed up the progress within these fields and assist in creating a more sustainable humanity. Note that diverse ML methods applied to gasification exist, including supervised, unsupervised and hybrid techniques. A complete description of this broad and evolving topic cannot be accomplished in one review paper. A follow-on review could include other methods such as support vector machines (SVMs), random forests (RFs), Naïve Bayes classifications, etc.

Author Contributions

Conceptualization, O.S. and E.M.; methodology, O.S. and E.M.; formal analysis, O.S. and E.M.; writing-original draft preparation, O.S.; writing-review and editing, E.M. and T.S.; All authors have read and agreed to the published version of the manuscript.

Competing Interests

The authors have declared that no competing interests exist.

Disclaimer

The views expressed in this paper are those of the authors and do nor reflect the official policy or position of the U.S. Air Force, the U.S. Department of Defense, or the U.S. Government.

References

1. Brunner PH, Rechberger H. Waste to energy – key element for sustainable waste management. Waste Manag. 2015; 37: 3-12.
2. Malkow T. Novel and innovative pyrolysis and gasification technologies for energy efficient and environmentally sound MSW disposal. Waste Manag. 2004; 24: 53-79.
3. Leckner B. Process aspects in combustion and gasification waste-to-energy (WtE) units. Waste Manag. 2015; 37: 13-25.
4. Arena U. Process and technological aspects of municipal solid waste gasification. A review. Waste Manag. 2012; 32: 625-639.
5. Lombardi L, Carnevale E, Corti A. A review of technologies and performances of thermal treatment systems for energy recovery from waste. Waste Manag. 2015; 37: 26-44.
6. Veses A, Sanahuja-Parejo O, Martínez I, Callén MS, López JM, García T, et al. A pyrolysis process coupled to a catalytic cracking stage: A potential waste-to-energy solution for mattress foam waste. Waste Manag. 2021; 120: 415-423.
7. Nanda S, Berruti F. Municipal solid waste management and landfilling technologies: A review. Environ Chem Lett. 2021; 19: 1433-1456.
8. Klinghoffer NB, Castaldi MJ. Gasification and pyrolysis of municipal solid waste (MSW). In: Waste to energy conversion technology. Cambridge: Woodhead Publishing Limited; 2013. pp.146-176.

9. Hasan MM, Rasul MG, Khan MMK, Ashwath N, Jahirul MI. Energy recovery from municipal solid waste using pyrolysis technology: A review on current status and developments. Renew Sust Energ Rev. 2021; 145: 111073.

10. Sun Y, Qin Z, Tang Y, Huang T, Ding S, Ma X. Techno-environmental-economic evaluation on municipal solid waste (MSW) to power/fuel by gasification-based and incineration-based routes. J Environ Chem Eng. 2021; 9: 106108.

11. Pandey DS, Das S, Pan I, Leahy JJ, Kwapinski W. Artificial neural network based modelling approach for municipal solid waste gasification in a fluidized bed reactor. Waste Manag. 2016; 58: 202-213.

12. Baruah D, Baruah DC, Hazarika MK. Artificial neural network based modeling of biomass gasification in fixed bed downdraft gasifiers. Biomass Bioenergy. 2017; 98: 264-271.

13. Puig-Arnavat M, Hernández JA, Bruno JC, Coronas A. Artificial neural network models for biomass gasification in fluidized bed gasifiers. Biomass Bioenergy. 2013; 49: 279-289.

14. Wen HT, Lu JH, Phuc MX. Applying artificial intelligence to predict the composition of syngas using rice husks: A comparison of artificial neural networks and gradient boosting regression. Energies. 2021; 14: 2932.

15. Sun Y, Liu L, Wang Q, Yang X, Tu X. Pyrolysis products from industrial waste biomass based on a neural network model. J Anal Appl Pyrolysis. 2016; 120: 94-102.

16. Vellekoop EC. Artificial neural networks for determining the optimal process conditions of a gasification process. Delft: Delft University of Technology; 2016.

17. Narnaware SL, Panwar NL. Biomass gasification for climate change mitigation and policy framework in India: A review. Bioresour Technol Rep. 2022; 17: 100892.

18. Van Ommen JR, de Jong W. Biomass as a sustainable energy source for the future: Fundamentals of conversion processes. Hoboken: John Wiley & Sons; 2014.

19. Basu P. Biomass gasification, pyrolysis and torrefaction: Practical design and theory. 2nd Ed. Elsevier Science; 2013. pp.1-530.

20. Wang L, Weller CL, Jones DD, Hanna MA. Contemporary issues in thermal gasification of biomass and its application to electricity and fuel production. Biomass Bioenergy. 2008; 32: 573-581.

21. Kargbo HO, Zhang J, Phan AN. Optimisation of two-stage biomass gasification for hydrogen production via artificial neural network. Appl Energy. 2021; 302: 117567.

22. Liu B, Ji S. Comparative study of fluidized-bed and fixed-bed reactor for syngas methanation over Ni-W/TiO_2-SiO_2 catalyst. J Energy Chem. 2013; 22: 740-746.

23. Basu P. Design of biomass gasifiers. In: Biomass gasification, pyrolysis and torrefaction. Elsevier Science; 2013. pp.249-313.

24. Breault RW. Gasification processes old and new: A basic review of the major technologies. Energies. 2010; 3: 216-240.

25. Suksankraisorn K, Patumsawad S, Fungtammasan B. Co-firing of Thai lignite and municipal solid waste (MSW) in a fluidised bed: Effect of MSW moisture content. Appl Therm Eng. 2010; 30: 2693-2697.

26. Boehm RC, Yang Z, Bell DC, Feldhausen J, Heyne JS. Lower heating value of jet fuel from hydrocarbon class concentration data and thermo-chemical reference data: An uncertainty quantification. Fuel. 2022; 311: 122542.

27. Simeons C. Gasification of coal. Coal: Its role in tomorrow's technology. Oxford: Pergamon Press; 1978. pp.142-186.

28. Robertson EE, Wood RD. 38 - Pyrolytic gasification of renewable biomass resources. In: Solar energy conversion. Oxford: Pergamon Press; 1979. pp.1059-1089.

29. Banapurmath NR, Yaliwal VS, Adaganti SY, Halewadimath SS. Chapter 11 - Power generation from renewable energy sources derived from biodiesel and low energy content producer gas for rural electrification. In: Energy from toxic organic waste for heat and power generation. Sawston, Cambridge: Woodhead Publishing; 2019. pp.151-194.

30. Hwang IS, Sohn J, Lee UD, Hwang J. CFD-DEM simulation of air-blown gasification of biomass in a bubbling fluidized bed gasifier: Effects of equivalence ratio and fluidization number. Energy. 2021; 219: 119533.

31. Zhang J, Liu J, Evrendilek F, Zhang X, Buyukada M. TG-FTIR and PY-GC/MS analyses of pyrolysis behaviors and products of cattle manure in CO_2 and N_2 atmospheres: Kinetic, thermodynamic, and machine-learning models. Energy Convers Manage. 2019; 195: 346-359.

32. Wen S, Buyukada M, Evrendilek F, Liu J. Uncertainty and sensitivity analyses of co-combustion/pyrolysis of textile dyeing sludge and incense sticks: Regression and machine-learning models. Renew Energ. 2020; 151: 463-474.

33. Pathy A, Meher S, Balasubramanian P. Predicting algal biochar yield using eXtreme Gradient Boosting (XGB) algorithm of machine learning methods. Algal Res. 2020; 50: 102006.

34. Özveren U, Kartal F, Sezer S, Özdoğan ZS. Investigation of steam gasification in thermogravimetric analysis by means of evolved gas analysis and machine learning. Energy. 2022; 239: 122232.

35. Seo MW, Lee SH, Nam H, Lee D, Tokmurzin D, Wang S, et al. Recent advances of thermochemical conversion processes for biorefinery. Bioresour Technol. 2022; 343: 126109.

36. Liu S, Ji H, Hou Z, Zuo J, Fan L. Data-driven online modelling for a UGI gasification process using modified lazy learning with a relevance vector machine. Int J Appl Math Comput Sci. 2021; 31: 321-335.

37. Cheng F, Small AA, Colosi LM. The levelized cost of negative CO_2 emissions from thermochemical conversion of biomass coupled with carbon capture and storage. Energy Convers Manage. 2021; 237: 114115.

38. Ayodele BV, Mustapa SI, Kanthasamy R, Zwawi M, Cheng CK. Modeling the prediction of hydrogen production by co-gasification of plastic and rubber wastes using machine learning algorithms. Int J Energy Res. 2021; 45: 9580-9594.

39. Wang Z, Huang S, Wen G, Liu Q, Tang P. Thermal conductivity prediction and structure-property relationship of CaO-SiO_2-Al_2O_3 ternary system: A combination of molecular dynamics simulations and machine learning. J Mol Liq. 2021; 324: 114697.

40. Wang Y, Liao Z, Mathieu S, Bin F, Tu X. Prediction and evaluation of plasma arc reforming of naphthalene using a hybrid machine learning model. J Hazard Mater. 2021; 404: 123965.

41. Ascher S, Watson I, You S. Machine learning methods for modelling the gasification and pyrolysis of biomass and waste. Renew Sustain Energ Rev. 2022; 155: 111902.

42. Joshi LM, Bharti RK, Singh R. Internet of things and machine learning-based approaches in the urban solid waste management: Trends, challenges, and future directions. Expert Syst. 2022; 39: e12865.

43. Shin Y, Shin D. Deep learning and AutoML for dynamic modeling of LNG regasification process using seawater. Comput Aided Chem Eng. 2021; 50: 1617-1622.

44. Das B, Patgiri R, Bandyopadhyay B, Balas VE. Modeling, simulation and optimization: Proceedings of CoMSO 2020. Springer Nature; 2021.

45. Okai K, Fujiwara H, Nagai K, Oinuma H, Makida M, Shimodaira K, et al. Combustion tests using a single combustor model and a jet engine of bio-derived aviation fuel produced through integrated process of woody biomass gasification and Fischer-Tropsch synthesis. In AIAA Scitech 2021 Forum. 2021. pp.2021-2036.

46. Bahadar A, Kanthasamy R, Sait HH, Zwawi M, Algarni M, Ayodele BV, et al. Elucidating the effect of process parameters on the production of hydrogen-rich syngas by biomass and coal co-gasification techniques: A multi-criteria modeling approach. Chemosphere. 2022; 287: 132052.

47. Rzychoń M, Żogała A, Róg L. An interpretable extreme gradient boosting model to predict ash fusion temperatures. Minerals. 2020; 10: 487.

48. Kozlov AN, Tomin NV, Sidorov DN, Lora EES, Kurbatsky VG. Optimal operation control of PV-biomass gasifier-diesel-hybrid systems using reinforcement learning techniques. Energies. 2020; 13: 2632.

49. Elmaz F, Yücel Ö, Mutlu AY. Predictive modeling of biomass gasification with machine learning-based regression methods. Energy. 2020; 191: 116541.

50. Xiao Y, Yin H, Xia K, Zhang Y, Qi H. Utilization of CNN-LSTM model in prediction of multivariate time series for UCG. Proceedings of ML4CS 2020: Machine Learning for Cyber Security; 2020 October 8-10; Guangzhou, China. Cham: Springer.

51. Sustainable Waste Management Workshop: Microplastics in the Environment 2020. Proceedings of Sustainable Waste Management Workshop; 2020 January 7-9; Create Tower NUS, Singapore. New York: AiCHE.

52. Yang X, Ma Z, Shen H, Chen H. Fault diagnosis of airflow jamming fault in double circulating fluidized bed based on multi-scale feature energy and KELM. CIESC J. 2019; 70: 2616-2625.

53. Ozbas EE, Aksu D, Ongen A, Aydin MA, Ozcan HK. Hydrogen production via biomass gasification, and modeling by supervised machine learning algorithms. Int J Hydrogen Energy. 2019; 44: 17260-17268.

54. Xiao Y, Yin J, Hu Y, Wang J, Yin H, Qi H. Monitoring and control in underground coal gasification: Current research status and future perspective. Sustainability. 2019; 11: 217.

55. Kačur J, Durdán M, Laciak M, Flegner P. A comparative study of datadriven modeling methods for softsensing in underground coal gasification. Acta Polytech. 2019; 59: 322-351.

56. Li J, Suvarna M, Pan L, Zhao Y, Wang X. A hybrid data-driven and mechanistic modelling approach for hydrothermal gasification. Appl Energy. 2021; 304: 117674.

57. Mutlu AY, Yucel O. An artificial intelligence based approach to predicting syngas composition for downdraft biomass gasification. Energy. 2018; 165: 895-901.

58. Ögren Y, Tóth P, Garami A, Sepman A, Wiinikka H. Development of a vision-based soft sensor for estimating equivalence ratio and major species concentration in entrained flow biomass gasification reactors. Appl Energy. 2018; 226: 450-460.

59. Wang KC, Shang C, Ke WS. Automatic structure and parameters tuning method for deep neural network soft sensor in chemical industries. CIESC J. 2018; 69: 900-906.

60. Misener R, Olofsson S, Wiebe J, Deisenroth MP. Gaussian processes for hybridizing analytical & data-driven decision-making. Proceedings of 2018 AIChE Annual Meeting; 2018 October 28-November 2; Pittsburgh, PA, USA.

61. Aznan KA, Khan S, Yaacob M, Khalifa OO, Aboadla E, Tohtayong M, et al. Integrated renewable energy micro-grid for meeting peak hours demand. Proceedings of the 5th IET International Conference on Clean Energy and Technology, CEAT 2018; 2018 September 5-6; Kuala Lumpur, Malaysia. Stevenage: Institution of Engineering and Technology.

62. Kačur J, Laciak M, Durdán M, Flegner P. Utilization of machine learning method in prediction of ucg data. Proceedings of 2017 18th International Carpathian Control Conference (ICCC); 2017 May 28-31; Sinaia, Romania. New York: IEEE.

63. Igathinathane C, Ulusoy U. Machine vision methods based particle size distribution of ball- and gyro-milled lignite and hard coal. Powder Technol. 2016; 297: 71-80.

64. 59th ISA Power Industry Division Symposium 2016, POWID 2016. Proceedings of the 59th Annual ISA POWID Symposium; 2016 June 27-30; Charlotte, North Carolina, USA. San Francisco: Curran Associates, Inc.

65. Liu S, Hou Z, Yin C. Data-driven modeling for fixed-bed intermittent gasification processes by enhanced lazy learning incorporated with relevance vector machine. Proceedings of the 11th IEEE International Conference on Control & Automation (ICCA); 2014 June 18-20; Taichung, Taiwan, China. New York: IEEE.

66. Xu W, Wang R, Gu X, Sun Y. Assessment of Texaco syngas components using extreme learning machine based quantum neural network. Proceedings of ICSEE 2012: Intelligent Computing for Sustainable Energy and Environment; 2012 September 12-13; Shanghai, China. Berlin/Heidelberg: Springer.

67. Li J, Pan L, Suvarna M, Wang X. Machine learning aided supercritical water gasification for H_2-rich syngas production with process optimization and catalyst screening. Chem Eng J. 2021; 426: 131285.

68. Binns M, Ayub HMU. Model reduction applied to empirical models for biomass gasification in downdraft gasifiers. Sustainability. 2021; 13: 12191.

69. Chen E, Deng R, Wang Z, Fang Z. Spatial feature learning based gaussian process regression for blast furnace raceway temperature prediction. Proceedings of 2021 International Conference on Electronic Information Engineering and Computer Science (EIECS); 2021 September 23-26; Changchun, China. New York: IEEE.

70. Zhao S, Li J, Chen C, Yan B, Tao J, Chen G. Interpretable machine learning for predicting and evaluating hydrogen production via supercritical water gasification of biomass. J Clean Prod. 2021; 316: 128244.

71. Gopirajan PV, Gopinath KP, Sivaranjani G, Arun J. Optimization of hydrothermal gasification process through machine learning approach: Experimental conditions, product yield and pollution. J Clean Prod. 2021; 306: 127302.

72. Sezer S, Özveren U. Investigation of syngas exergy value and hydrogen concentration in syngas from biomass gasification in a bubbling fluidized bed gasifier by using machine learning. Int J Hydrogen Energy. 2021; 46: 20377-20396.

73. Kartal F, Özveren U. A deep learning approach for prediction of syngas lower heating value from CFB gasifier in Aspen plus®. Energy. 2020; 209: 118457.

74. Hagan MT, Demuth HB, Beale MH, De Jesús O. Neural Network Design. 2nd Ed. Martin Hagan; 2014.

75. Krzywanski J, Fan H, Feng Y, Shaikh AR, Fang M, Wang Q. Genetic algorithms and neural networks in optimization of sorbent enhanced H_2 production in FB and CFB gasifiers. Energy Convers Manage. 2018; 171: 1651-1661.

76. Cao H, Xin Y, Yuan Q. Prediction of biochar yield from cattle manure pyrolysis via least squares support vector machine intelligent approach. Bioresour Technol. 2016; 202: 158-164.

77. George J, Arun P, Muraleedharan C. Assessment of producer gas composition in air gasification of biomass using artificial neural network model. Int J Hydrogen Energy. 2018; 43: 9558-9568.

78. Safarian S, Ebrahimi Saryazdi SM, Unnthorsson R, Richter C. Artificial neural network integrated with thermodynamic equilibrium modeling of downdraft biomass gasification-power production plant. Energy. 2020; 213: 118800.

79. Serrano García D, Golpour I, Sánchez Delgado S. Predicting the effect of bed materials in bubbling fluidized bed gasification using artificial neural networks (ANNs) modeling approach. 2020; 266: 117021.

80. Shenbagaraj S, Sharma PK, Sharma AK, Raghav G, Kota KB, Ashokkumar V. Gasification of food waste in supercritical water: An innovative synthesis gas composition prediction model based on artificial neural networks. Int J Hydrogen Energy. 2021; 46: 12739-12757.

81. Sunphorka S, Chalermsinsuwan B, Piumsomboon P. Artificial neural network model for the prediction of kinetic parameters of biomass pyrolysis from its constituents. Fuel. 2017; 193: 142-158.

82. Yucel O, Aydin ES, Sadikoglu H. Comparison of the different artificial neural networks in prediction of biomass gasification products. Int J Energy Res. 2019; 43: 5992-6003.

83. Ma H, Yang X, Mao J, Zheng H. The energy efficiency prediction method based on gradient boosting regression tree. Proceedings of 2018 2nd IEEE Conference on Energy Internet and Energy System Integration (EI2); 2018 October 20-22; Beijing, China. New York: IEEE.

84. Xue P, Lei Y, Li Y. Research and prediction of Shanghai-Shenzhen 20 index based on the support vector machine model and gradient boosting regression tree. Proceedings of 2020 International Conference on Intelligent Computing, Automation and Systems (ICICAS); 2020 December 11-13; Chongqing, China. New York: IEEE.

85. Huaiyu L, Hongli W, Guanmin L, Shuangmei L, Jialiang G. Study on urban wastewater discharge forecasting and influence factors analysis based on stochastic gradient regression. Proceedings of 2009 Third International Symposium on Intelligent Information Technology Application; 2009 November 21-22; Nanchang, China. New York: IEEE.

86. Konstantinov AV, Utkin LV. Interpretable machine learning with an ensemble of gradient boosting machines. Knowl Based Syst. 2021; 222: 106993.

87. Li J, Pan L, Suvarna M, Tong YW, Wang X. Machine learning prediction of syngas composition of hydrothermal gasification from wet organic wastes. Proceedings of International Conference on Applied Energy 2020; 2020 December 1-10; Bangkok, Thailand.

Enjoy *JEPT* by:

1. Submitting a manuscript
2. Joining in volunteer reviewer bank
3. Joining Editorial Board
4. Guest editing a special issue

For more details, please visit:
http://www.lidsen.com/journal/jept